Supporting Information

Quantitative Imaging of Ion Transport through Single Nanopores by High-Resolution Scanning Electrochemical Microscopy

Mei Shen, Ryoichi Ishimatsu, Jiyeon Kim, and Shigeru Amemiya*

Department of Chemistry, University of Pittsburgh, 219 Parkman Avenue, Pittsburgh, Pennsylvania, 15260

Chemicals. Tetradodecylammonium (TDDA) bromide, tetrabutylammonium chloride (TBACl), 1,2-dichloroethane, potassium chloride, and *N*-dimethyltrimethyl silylamine were purchased from Sigma-Aldrich (Saint Louis, MO). Potassium tetrakis(pentafluorophenyl)borate (TFAB) was obtained from Boulder Scientific Company (Mead, CO). Isopropyl alcohol from J. T. Baker (Phillipsburg, NJ). All reagents were used as received. The TFAB salt of TDDA was prepared by metathesis.[S-1] 10 mM TBACl was dissolved in 18.3 MΩ cm deionized water (Nanopure, Barnstead, Dubuque, IA) with 0.3 M KCl. The resulting solution was passed through a 0.2 μm filter (Fisher Scientific, Hanover Park, IL) before its use for SECM imaging.

SEM of Nanopipets. A nanopipet was pulled [S-2] as reported elsewhere and coated with a thin Pd film by a high-resolution sputter coater (Cressington 208HR, Ted Pella, Redding, CA) at a working distance of 4 cm with 20 mA for 5 s. The orifice of a Pd-coated nanopipet was observed by field-emission SEM (model XL-30, Philips Electron Optics, Eindhoven, Netherlands) under 15 kV electron beam.

Membrane Characterization and Pretreatment. A pnc-Si membrane (US100-P30Q33, TEMwindows, West Henrietta, NY) was characterized and cleaned as follow. The distribution of pore diameter was determined from the TEM image of a nanomembrane (Figure 1A). The pore diameter is the average of major and minor axes obtained by fitting every pore as an ellipse as reported elsewhere.[S-3] For cleaning, the membrane was soaked in a piranha solution (1:1 volume ratio sulfuric acid: hydrogen peroxide) for 4–6 min, in water for 4–11 min, and then in isopropyl alcohol for 3 min. The cleaned membrane was placed into the electrochemical cell filled with water, which was replaced with 24 ml of 10 mM TBACl in 0.3 M KCl. The position of the membrane was fixed by screwing two glass slides from opposite sides onto the membrane.

SECM Imaging. The setup of our SECM system is detailed elsewhere.[S-2] Briefly, a home-built SECM stage was used for tip positioning while the potentiostat of CHI 900 (CH Instruments, Austin, TX) was used for recording the tip current in a two electrode cell with Ag/AgCl and Pt electrodes in outer aqueous and inner organic phases, respectively. The *x*, *y*, and *z*-positions of a nanopipet tip were roughly controlled using the micrometers (SM-25 for *z*-axis and AJS100-1 for *x*, *y*-axes, Newport, Irvine, CA) of the SECM stage (M-462, Newport), which is also equipped with piezoelectric positioners with closed-loop capacitive sensors for nanoscale tip positioning. Specifically, a *z*-axis positioner, P-621.ZCD, was controlled by E-665CR while two E-625.CR controllers were employed for *x*, *y*-axis positioners, P-620.2CD, where all positioners and controllers are from PI (Auburn, MA). A Labview program was written to control the positioners in the drift compensation mode, which eliminates drift in the digital-analog converters on the main board of the controllers. The microscope stage was accommodated in an isothermal chamber,[S-2] which was placed in a faraday cage on a vibration isolation table (63-533, TMC, Peabody, MA).

As far as we imaged the small area of a pnc-Si membrane using a sharp tip with small *RG*, there was no significant change in the tip–substrate distance or the tip–substrate contact, which can be caused by their imperfect alignment. As schematically shown in Figure S-1A, we were able to achieve a sufficiently parallel alignment between the substrate surface and the tip surface simply using a bubble level because (i) dimensions of 280 nm × 500 nm for the whole SECM image in Figure 3A are only ~8 and ~15 times larger than an inner tip diameter of 34 nm and (ii) the sharp tip has a small *RG* value of 1.4. Noticeably, the parallel alignment required for constant-height imaging in this work is very similar to the parallel alignment required for perpendicularly approaching a typical SECM nanotip with a large *RG* value of ~10 near the substrate surface without contact (Figure S-1B), which was also achieved using a bubble level.[S-4]

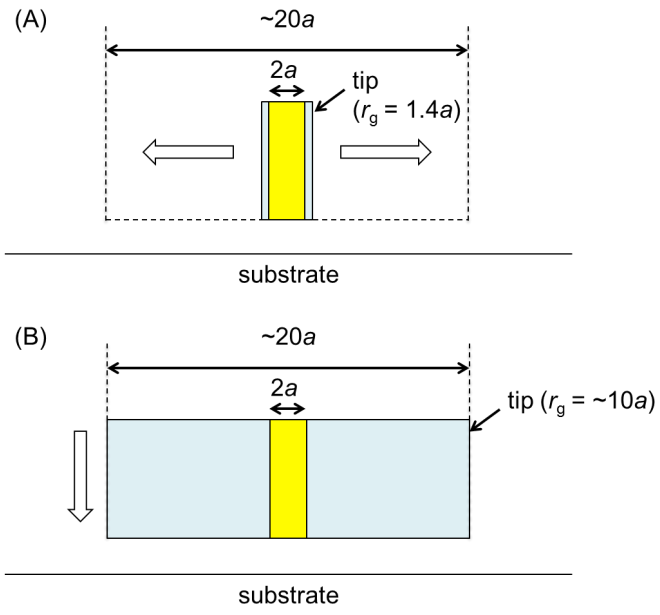

Figure S-1. Parallel alignment between the tip surface and the substrate surface required for (A) imaging a small area using a sharp tip with *RG* = 1.4 and (B) positioning a typical tip with *RG* = ~10 near the substrate surface.

Prior to imaging, the tip was brought in close proximity to a nanopore membrane at (x, y) = (0, 0) using the feedback mode of SECM, and held at a constant height from the membrane surface. Then, the tip was scanned in x-direction with a step size of 4 nm in 70 steps, thereby resulting in a travel distance of 280 nm (Figure S-2). After each line scan, the x-position of the tip was returned to 0 nm and its y position was shifted by 5 nm, which was followed by the next line scan from x = 0 nm to x = 280 nm. The line scan in x-direction was repeated from y = 0 nm to y = 500 nm at every 5 nm for 100 steps. Overall, it took ~12 minutes (Figure 3B) to obtain the 280 nm × 500 nm image with 71 × 101 data points.

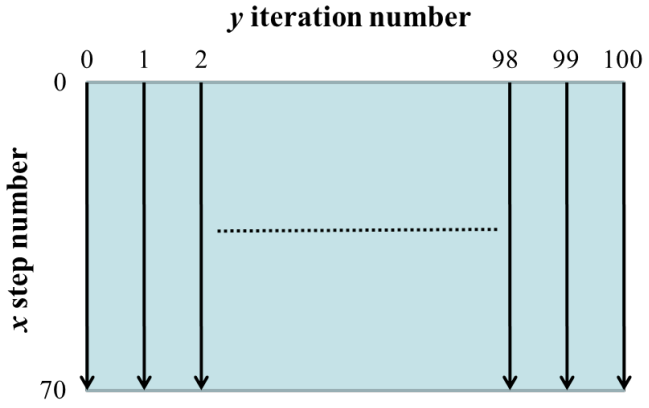

Figure S-2. Scheme of lateral scanning directions.

Finite Element Simulation. The simulation report generated by COMSOL Multiphysics finite element package (version 3.5a, COMSOL, Inc., Burlington, MA) is attached. In this simulation, an SECM diffusion problem with a disk-shaped tip over a nanopore as an elliptic cylinder is defined in Cartesian coordinates (Figure S-3). The origin of the coordinate axes is set at the center of the upper orifice of the nanopore. Initially, the solution phase contains a target ion at a bulk concentration of c^*. The diffusion of the target ion in the solution phase is defined by

$$\frac{\partial c}{\partial t} = D\left(\frac{\partial^2 c}{\partial x^2} + \frac{\partial^2 c}{\partial y^2} + \frac{\partial^2 c}{\partial z^2}\right) \qquad \text{(S-1)}$$

where c is the ion concentration at (x, y, z). Ion diffusion in the inner organic solution does not affect the tip current, which is limited by the diffusion of the traget ion in the outer aqueous solution. Accordingly, the zero ion concentration is used as the electrode surface boundary condition (red lines in Figure S-3). The membrane surface and pore wall are impermeable to an ion, which corresponds to zero flux perpendicluar to these boundaries (black bold lines). Boundary conditions at simulation space limits are given by the bulk concentration of the ion, c^* (blue lines). The simulation space is large enough to affect the simulated tip current less than 1.5 %.

Specifically, eq S-1 was solved using the approximate size of a nanopore, which is smaller by the tip diameter than the corresponding size in an SECM image (see main text). Then, pore size in the simulation was adjusted until experimental line scans in the image fit with simulation results (Figure 4A).

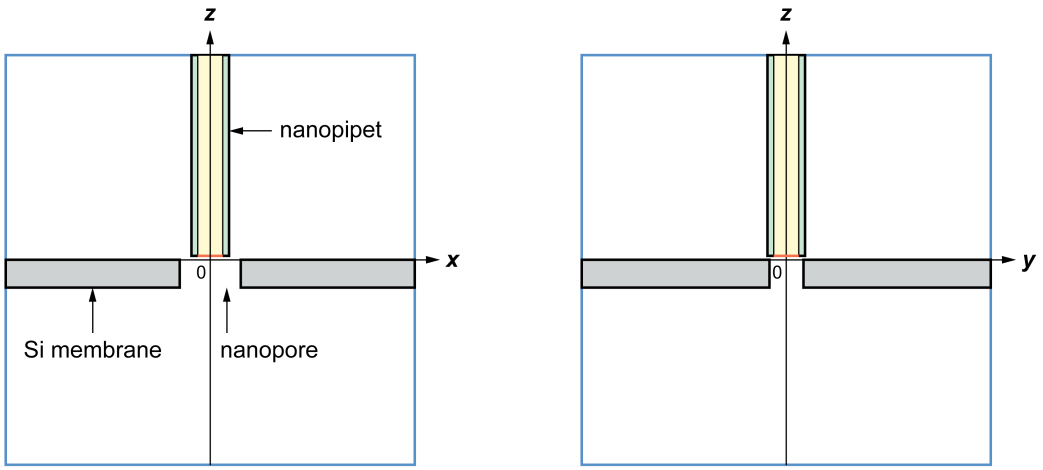

Figure S-3. Scheme of cross sections of simulation space at $y = 0$ (left) and $x = 0$ (right).

Effect of Pore Depth on Tip Current. The x-line scans over pore **7** at $\Delta y = 0$ were simulated using different pore depths (Figure S-4) to confirm its unique depth of 30 nm.

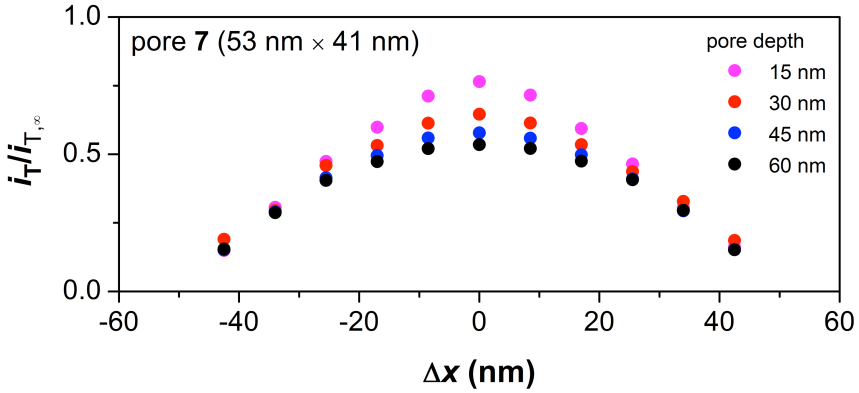

Figure S-4. Effect of pore depth on simulated current responses in x-line scans over pore **7** at $\Delta y = 0$ nm. See the legend of Figure 4 for other parameters.

REFERENCES

(S-1) Guo, J.; Amemiya, S. *Anal. Chem.* **2006**, *78*, 6893.

(S-2) Kim, J.; Shen, M.; Nioradze, N.; Amemiya, S. *Anal. Chem.* **2012**, *84*, 3489.

(S-3) Kim, E.; Xiong, H.; Striemer, C. C.; Fang, D. Z.; Fauchet, P. M.; McGrath, J. L.; Amemiya, S. *J. Am. Chem. Soc.* **2008**, *130*, 4230.

(S-4) Sun, P.; Mirkin, M. V. *Anal. Chem.* **2006**, *78*, 6526.

COMSOL Model Report

1. Table of Contents

2. Model Properties

Property	Value
Model name	
Author	
Company	
Department	
Reference	
URL	
Saved date	May 15, 2012 11:20:33 AM
Creation date	Jan 30, 2010 5:51:36 PM
COMSOL version	COMSOL 3.5.0.603

Application modes and modules used in this model:

- Geom1 (2D)
- Geom2 (2D)
- Geom3 (2D)
- Geom4 (2D)
- Geom5 (3D)
    - Diffusion (Chemical Engineering Module)

3. Geometry

Number of geometries: 5

3.1. Geom1

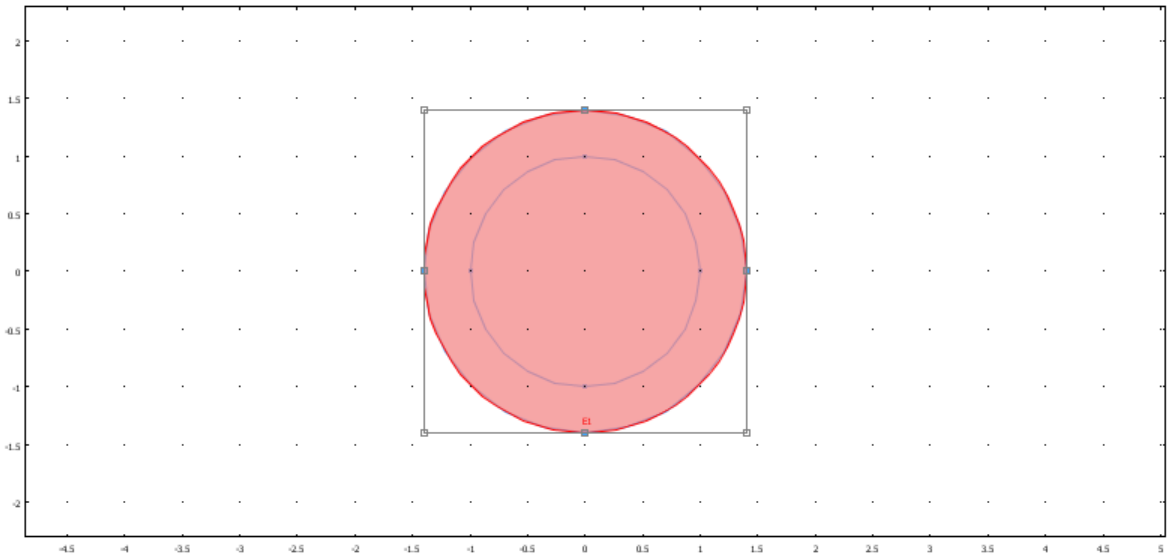

3.2. Geom2

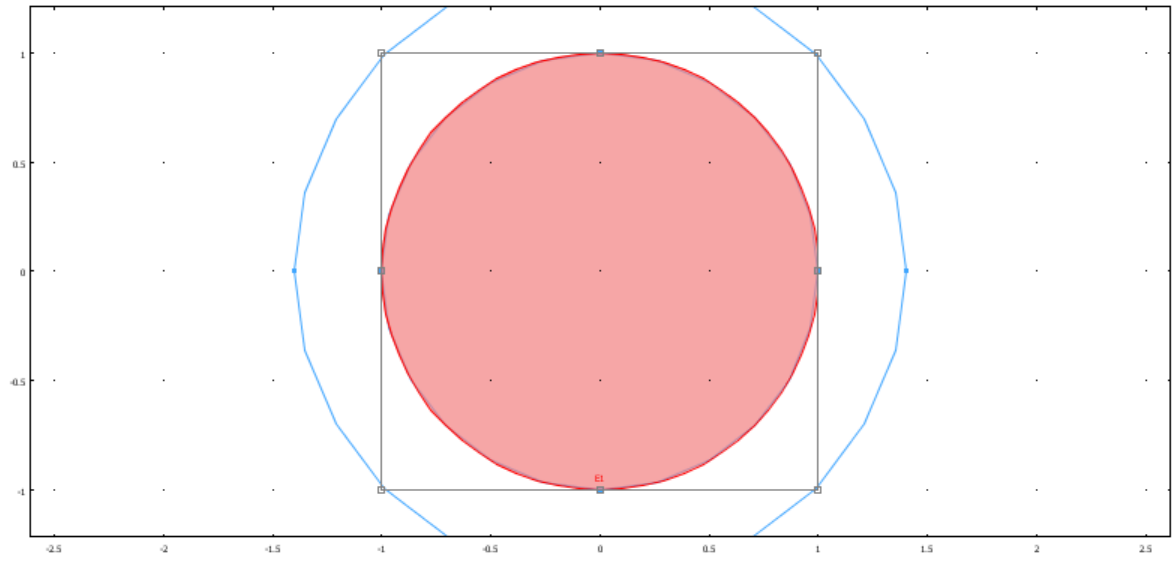

3.3. Geom3

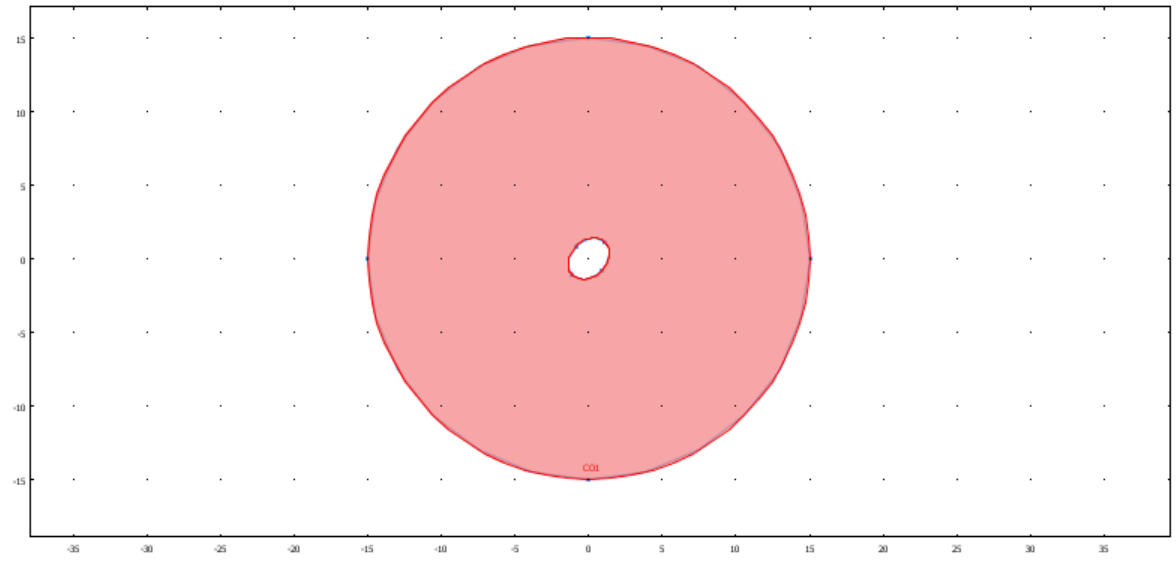

3.4. Geom4

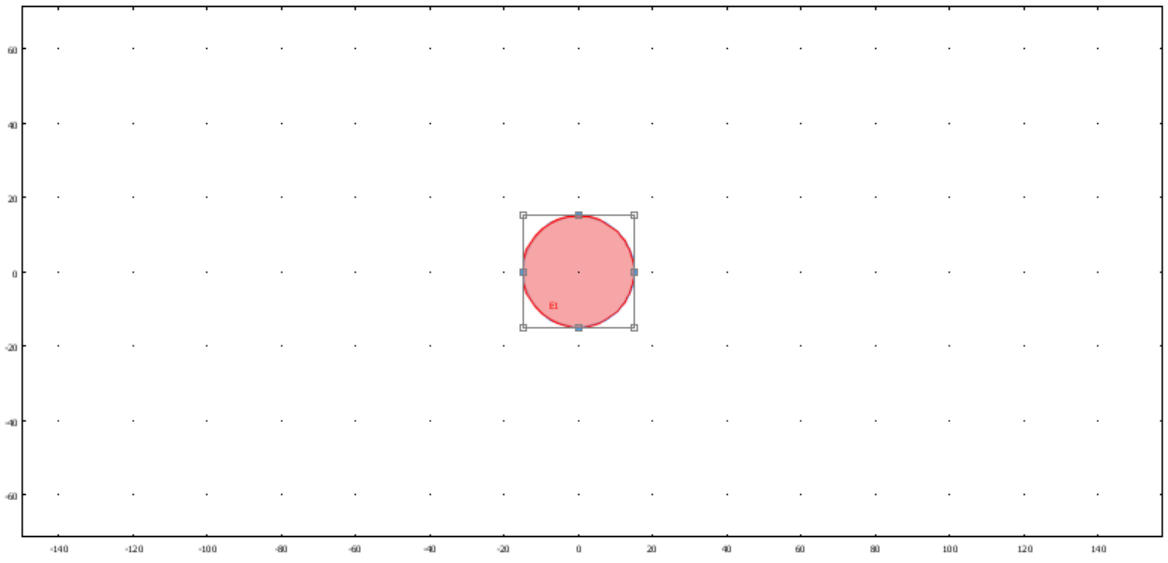
E1
60
40
20
0
-20
-40
-60
-140
-120
-100
-80
-60
-40
-20
0
20
40
60
80
100
120
140

3.5. Geom5

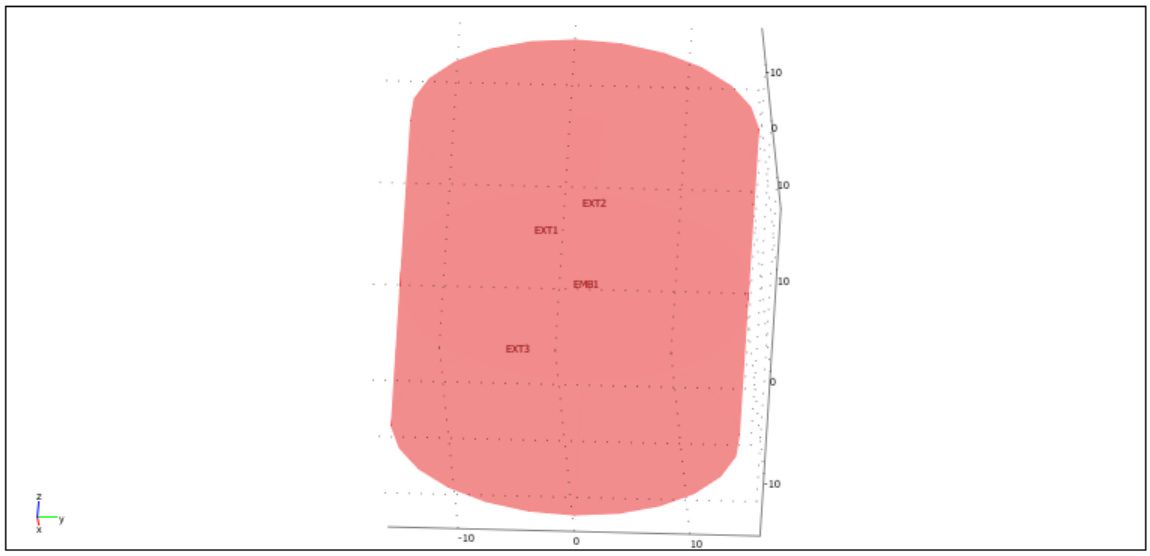

3.5.1. Point mode

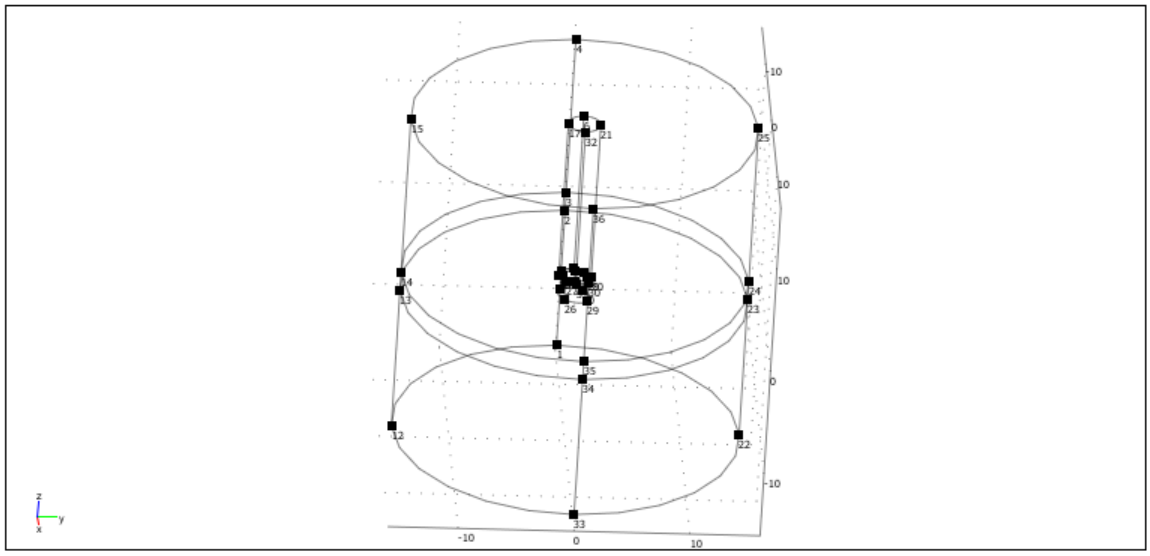

3.5.2. Edge mode

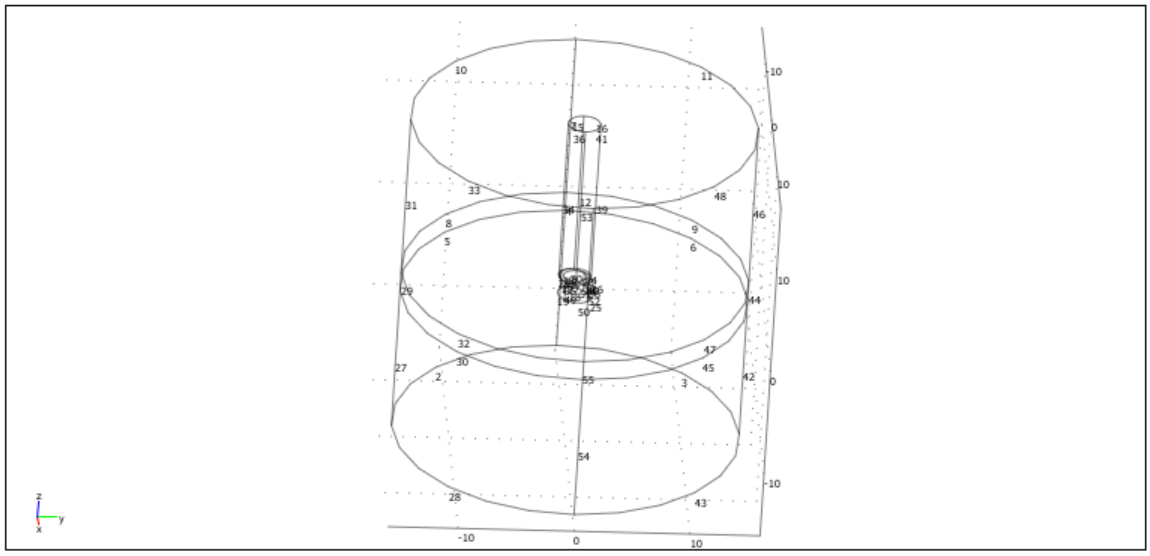

3.5.3. Boundary mode

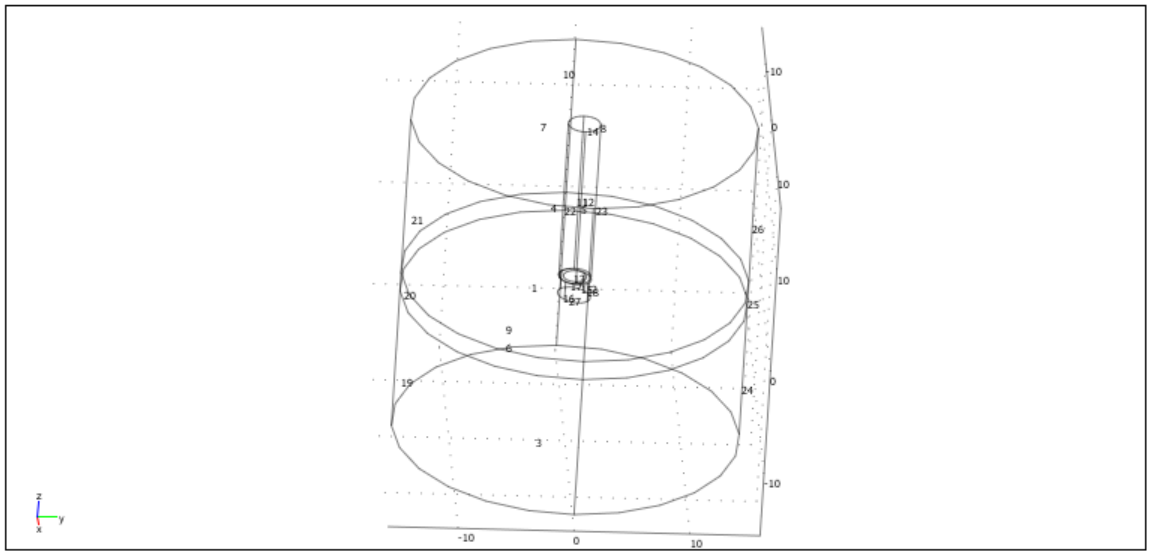

3.5.4. Subdomain mode

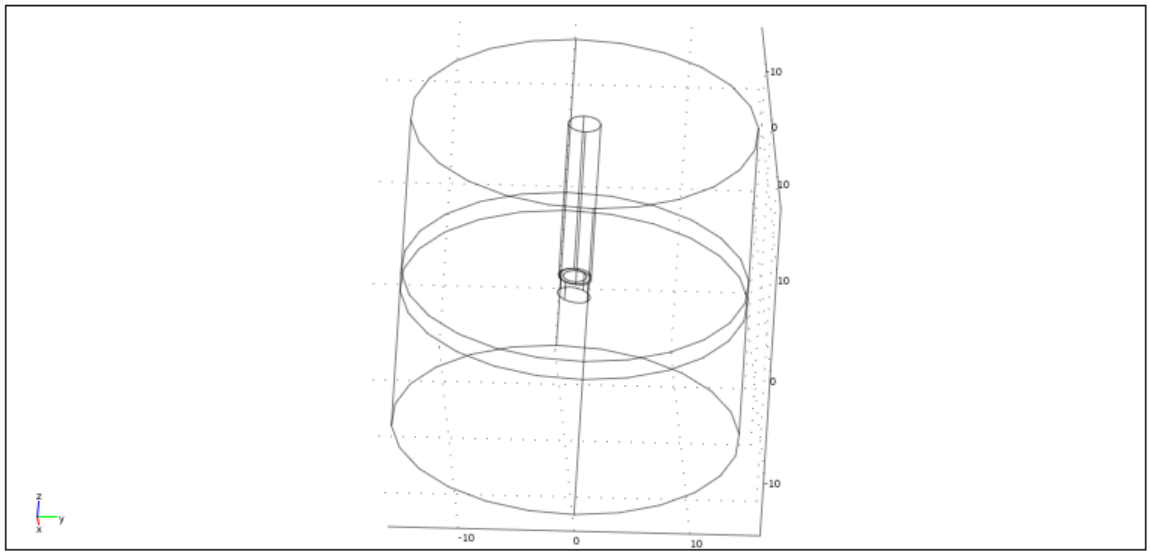

4. Geom1

Space dimensions: 2D

Independent variables: x, y, z

5. Geom2

Space dimensions: 2D

Independent variables: x, y, z

6. Geom3

Space dimensions: 2D

Independent variables: x, y, z

7. Geom4

Space dimensions: 2D

Independent variables: x, y, z

8. Geom5

Space dimensions: 3D

Independent variables: x, y, z

8.1. Mesh

8.1.1. Mesh Statistics

Number of degrees of freedom	250495
Number of mesh points	54195
Number of elements	318297
Tetrahedral	318297
Prism	0
Hexahedral	0
Number of boundary elements	27502
Triangular	27502
Quadrilateral	0
Number of edge elements	1660
Number of vertex elements	36
Minimum element quality	0.299
Element volume ratio	0

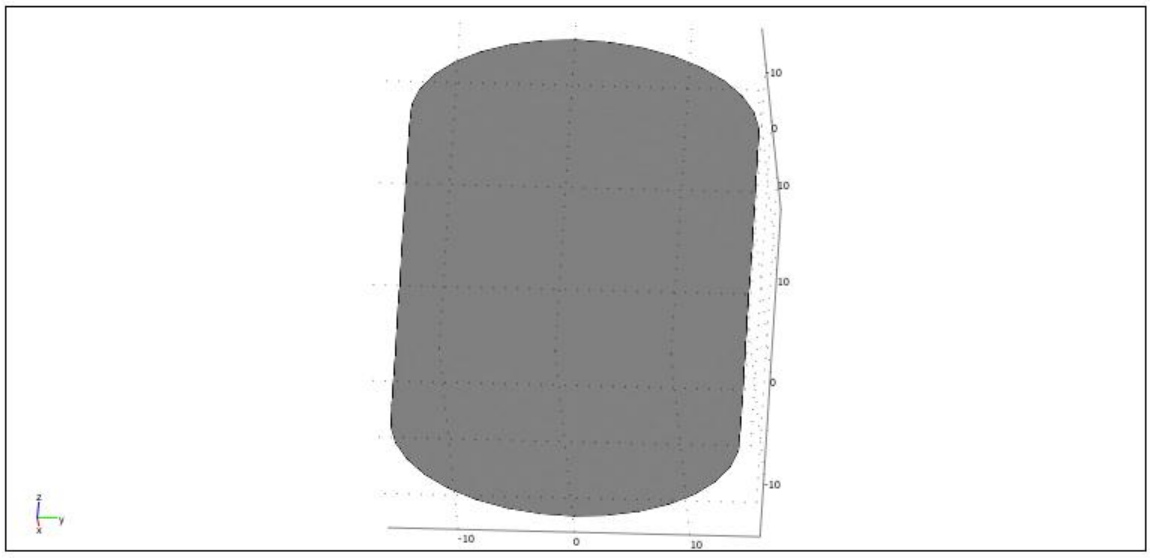

8.2. Application Mode: Diffusion (chdi)

Application mode type: Diffusion (Chemical Engineering Module)

Application mode name: chdi

8.2.1. Application Mode Properties

Property	Value
Default element type	Lagrange - Quadratic
Analysis type	Stationary
Equilibrium assumption	Off
Frame	Frame (xyz)
Weak constraints	Off
Constraint type	Ideal

8.2.2. Variables

Dependent variables: c

Shape functions: shlag(2,'c')

Interior boundaries not active

8.2.3. Boundary Settings

Boundary		1-3, 7-8, 10, 19, 21, 24, 26	6, 9, 11-13, 15-16, 18, 22-23, 27	17
Type		Concentration	Insulation/Symmetry	Concentration
Concentration (c0)	mol/m^3	**1**	0	0

8.2.4. Subdomain Settings

The subdomain settings only contain default values.

Subdomain initial value		1
Concentration, c (c)	mol/m^3	1

9. Solver Settings

Solve using a script: off

Analysis type	Stationary
Auto select solver	On
Solver	Stationary
Solution form	Automatic
Symmetric	auto
Adaptive mesh refinement	Off
Optimization/Sensitivity	Off
Plot while solving	Off

9.1. Direct (UMFPACK)

Solver type: Linear system solver

Parameter	Value
Pivot threshold	0.1
Memory allocation factor	0.7

9.2. Stationary

Parameter	Value
Linearity	Automatic
Relative tolerance	1.0E-6
Maximum number of iterations	25
Manual tuning of damping parameters	Off
Highly nonlinear problem	Off
Initial damping factor	1.0
Minimum damping factor	1.0E-4
Restriction for step size update	10.0

9.3. Advanced

Parameter	Value
Constraint handling method	Elimination
Null-space function	Automatic
Automatic assembly block size	On
Assembly block size	1000

Use Hermitian transpose of constraint matrix and in symmetry detection	Off
Use complex functions with real input	Off
Stop if error due to undefined operation	On
Store solution on file	Off
Type of scaling	Automatic
Manual scaling	
Row equilibration	On
Manual control of reassembly	Off
Load constant	On
Constraint constant	On
Mass constant	On
Damping (mass) constant	On
Jacobian constant	On
Constraint Jacobian constant	On

10. Postprocessing

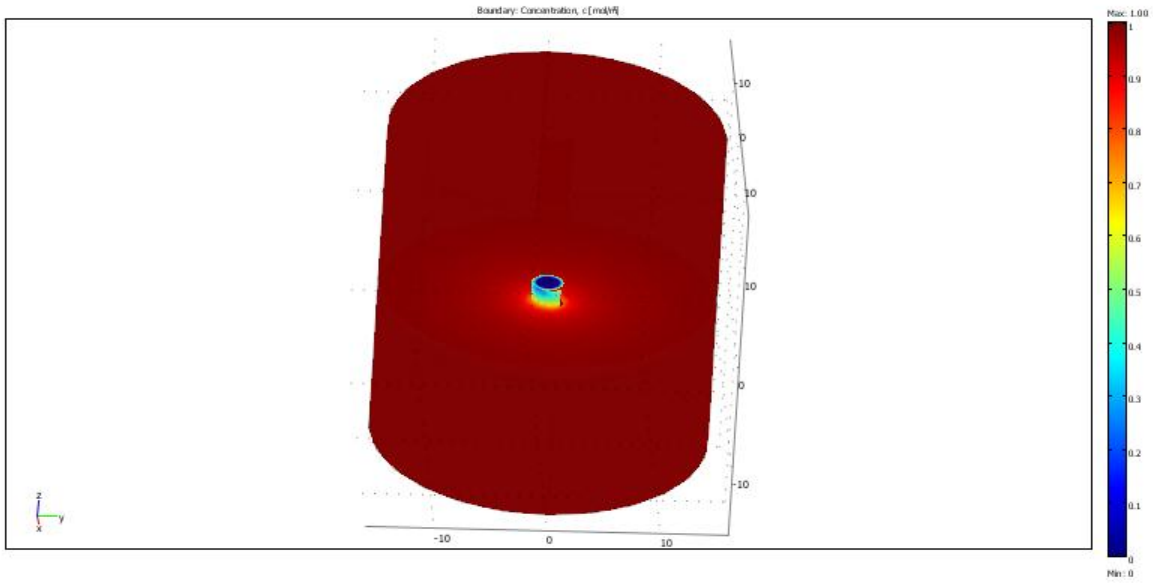

11. Variables

11.1. Boundary

11.1.1. Boundary 1-3, 6-13, 15-19, 21-24, 26-27

Name	Description	Unit	Expression
ndflux_c_chdi	Normal diffusive flux, c	mol/(m^2*s)	nx_chdi * dflux_c_x_chdi+ny_chdi * dflux_c_y_chdi+nz_chdi * dflux_c_z_chdi

11.1.2. Boundary 4-5, 14, 20, 25

Name	Description	Unit	Expression
ndflux_c_chdi	Normal diffusive flux, c	mol/(m^2*s)	

11.2. Subdomain

11.2.1. Subdomain 1

Name	Description	Unit	Expression
grad_c_x_chdi	Concentration gradient, c, x component	mol/m^4	cx
dflux_c_x_chdi	Diffusive flux, c, x component	mol/(m^2*s)	-Dxx_c_chdi * cx-Dxy_c_chdi * cy-Dxz_c_chdi * cz
grad_c_y_chdi	Concentration gradient, c, y component	mol/m^4	cy
dflux_c_y_chdi	Diffusive flux, c, y component	mol/(m^2*s)	-Dyx_c_chdi * cx-Dyy_c_chdi * cy-Dyz_c_chdi * cz
grad_c_z_chdi	Concentration gradient, c, z component	mol/m^4	cz
dflux_c_z_chdi	Diffusive flux, c, z component	mol/(m^2*s)	-Dzx_c_chdi * cx-Dzy_c_chdi * cy-Dzz_c_chdi * cz

grad_c_chdi	Concentration gradient, c	mol/m^4	sqrt(grad_c_x_chdi^2+grad_c_y_chdi^2+grad_c_z_chdi^2)
dflux_c_chdi	Diffusive flux, c	mol/(m^2*s)	sqrt(dflux_c_x_chdi^2+dflux_c_y_chdi^2+dflux_c_z_chdi^2)

11.2.2. Subdomain 2-3

Name	Description	Unit	Expression
grad_c_x_chdi	Concentration gradient, c, x component	mol/m^4	
dflux_c_x_chdi	Diffusive flux, c, x component	mol/(m^2*s)	
grad_c_y_chdi	Concentration gradient, c, y component	mol/m^4	
dflux_c_y_chdi	Diffusive flux, c, y component	mol/(m^2*s)	
grad_c_z_chdi	Concentration gradient, c, z component	mol/m^4	
dflux_c_z_chdi	Diffusive flux, c, z component	mol/(m^2*s)	
grad_c_chdi	Concentration gradient, c	mol/m^4	
dflux_c_chdi	Diffusive flux, c	mol/(m^2*s)	